

Hydrodynamics of Wet Type Dusty Gas Collector

Nasimbek Ergashev

On technical sciences, PhD. Ferghana polytechnic institute

Bakhtiyar Tilavaldiev

master teacher, Fergana Polytechnic Institute Republic of Uzbekistan

Annotation:

The article presents the results of an experimental study to determine the hydraulic resistance in a device in which the contact element generates a rotating current and to study its effect on the cleaning efficiency. The equation for determining the resistance coefficient of the contact element of the device is proposed and the correction coefficients are included, on the basis of which the values of the resistance coefficient are determined experimentally. The device used quartz sand and dolomite dust as samples to study the effect of working bodies on dusty gas flow. Comparative graphs were constructed for different values of variable factors of hydraulic resistance and its effect on cleaning efficiency and based on optimal parameters.

Keywords: flow rate, contact element, hydraulic resistance, resistance coefficient, quartz sand and dolomite dust, gas flow, liquid film, reference angle, blade, cleaning efficiency.

Introduction

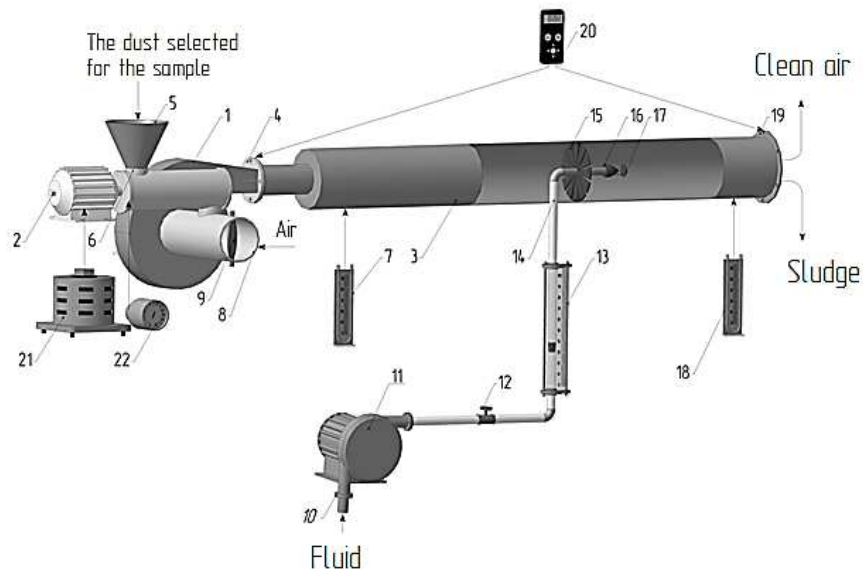
Industrial gases and air must be cleaned of dust in order to properly carry out technological processes in industrial enterprises. Mixers, dispersers, and most metabolic devices cannot function well without effective gas and dust removal schemes [1,2,3]. Currently, the following methods are used to clean dusty gas mixtures. 1. Sinking under the influence of gravity; 2. Drowning under the influence of centrifugal force; 3. Sedimentation in the field of electric and other forces; 4. Filtering; 5. Wet type of cleaning.

The most effective of these methods in the analysis is wet cleaning, which is currently widely used in industry, and a lot of research is being conducted in this area [4,5 and others]. For example, when using this type of device, a dusty stream will come into contact with a liquid in the form of a drop or film. According to the hydrophilic property, the powder adheres to the surface of the liquid and is expelled from the device with it. It also has the ability to capture very small particles (up to 0,1 μm) and high purification capacity (up to 99 %). However, the formation of liquid sludge when using this type of device and the extra energy required to re-purify it require research in this area.

One of the main technical requirements for the creation of new devices for the purification of dusty gases in wet water is to ensure high cleaning efficiency with minimal liquid consumption and thus reduce energy consumption.

Based on the above, a lot of research on the design of devices for cleaning and neutralization of wet dust gases in the wet method and their advantages and disadvantages were analyzed, based on which a design scheme of the device generating a contact element swirling current was developed [6] Figure 1.

In order to study the effect of the developed device hydraulic resistance on cleaning efficiency and energy consumption, its hydrodynamic regimes were theoretically and experimentally studied. Figure 2 shows the calculation scheme of the device.



1 – fan; 2 – electromotor; 3 – metal pipe; 4 – 10 – 19 Flanges; 5 – dust collector; 6 – dust supplier; 7,18 – Pito Prandl tube; 8-dusty air inlet lane 9 – stacker 11 – Pump; 12 – valve; 13 – rotameter; 14 – water supply pipe; 15 – gas flow-forming element; (fluorite) 16 – stutter of fluid ; 17 – water repellent; 20 – anemometer electronic meter; 21 – electromotor speed control apparatus; 22 – Instrument showing the velocity.

Figure 1. Total view of experimental device

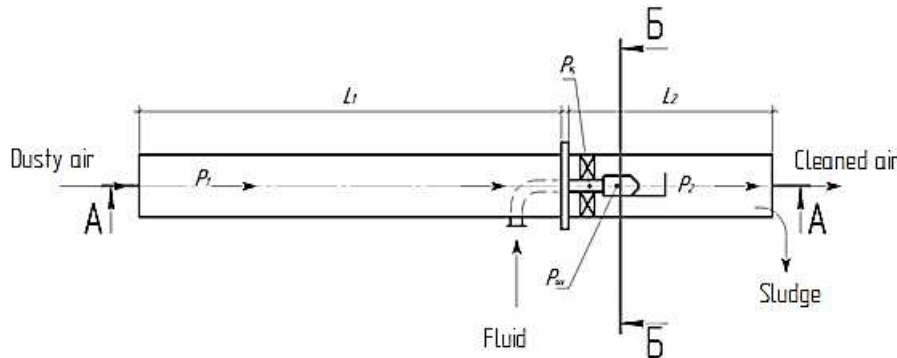


Figure 2. Determining scheme of contact element for creating swirling flow

Research theory and method

In theoretical studies, the total hydraulic resistances affecting the flow of dusty gas moving in a device in which the contact element generates a rotating flow can be written using the calculation equations given in the literature [7,8,9] and section A– A of the device calculation scheme, Pa

$$\Delta P = P_1 + P_2 \quad (1)$$

where P_1 – is the hydraulic resistance of the dust gas to the inlet pipe to the device and to the contact element forming the coil, which is determined by the following equation, Pa;

$$P_1 = \xi_1 \frac{v_1^2 \rho_{ar}}{2} \quad (2)$$

where v_1 – the velocity of the lost dust gas at the distance from the inlet pipe of the dusty gas to the device and the contact element forming the coil m/sec; ξ_1 – is the coefficient of local resistance of the dust gas to the device inlet pipe and the contact element forming the coil, which is determined by the following equation;

$$\xi_1 = \lambda \frac{l}{d_e} \quad (3)$$

where l – length of pipe, m; d_e – equivalent diameter of pipe, m; λ – Darcy coefficient, which is determined by the following equation;

$$\lambda = \frac{0,3164}{\text{Re}^{0.25}} \quad (4)$$

in this case, equation (3) looks like this;

$$\xi_1 = \frac{0,3164l}{d_e \sqrt[4]{\text{Re}}} \quad (5)$$

substituting equation (5) into Equation (2), we obtain the following equation, Pa;

$$P_1 = \frac{0,3164lv_1^2 \rho_{ar}}{2d_e \sqrt[4]{\text{Re}}} \quad (6)$$

P_2 – is the hydraulic resistance of the contact element forming the coupling, which is determined by the following equation, Pa;

$$P_2 = \xi_2 \frac{v_2^2 \rho_{ar}}{2} \quad (7)$$

where v_2 – the velocity of the gas lost due to the resistance of the contact element forming the coil, m/s; ξ_2 – is the coefficient of resistance of the contact element forming the coil, the determination of which is somewhat complicated and requires different deviations. It can only be determined experimentally on the device under experiment.

ρ_{ar} – is the density of a mixture of dust and gas, which is determined by the following equation, kg/m^3

$$\rho_{ar} = \rho_g + (\rho_{ch} \cdot \gamma) \quad (8)$$

where ρ_g – density of secondary gas, kg/m^3 ; ρ_{ch} – air density, kg/m^3 ; γ – the amount of secondary gas in the air, %.

Substituting equations (6) and (7) into equation (1), then the equation for determining the total hydraulic resistance of a device is given by Pa;

$$\Delta P = \frac{0,3164lv_1^2 \rho_{ar}}{2d_e \sqrt[4]{\text{Re}}} + \xi_2 \frac{v_2^2 \rho_{ar}}{2} \quad (9)$$

Through the resulting equation (9) we are able to determine the total hydraulic resistance in the device.

Determining the resistance coefficient ξ_2 in equation (9) is complex and requires different deviations. In this case, the following equation was obtained to determine the resistance coefficient by the ratio of the total surface area of the contact element paddles to the current-carrying surface, and the correction factor was introduced.

$$\Delta k \frac{4\pi R^2}{nab \sin \beta} \quad (10)$$

where n – number of blades; a, b – the length of the side of the blade; β – the angle of inclination of the open surface through which the gas flow passes through the contact element; Δk – is the correction factor, which is determined experimentally.

It can be seen from this equation that an increase in the slope angle of the open surface between the contact element blades leads to a decrease in the resistance coefficient.

Based on the above factors, by modifying Equation (9), it will be possible to determine the total hydraulic resistance of the device as follows, Pa;

$$\Delta P = \frac{0,3164l v_1^2 \rho_{ar}}{2d_e^4 \sqrt{\text{Re}}} + \Delta k \frac{2\pi R^2 v_2^2 \rho_{ar}}{nab \sin \beta} \quad (11)$$

The total hydraulic resistances acting on the fluid in section B-B of the device can be written as, Pa;

$$\Delta P_s = P_k + P_{sh} \quad (12)$$

where P_k – is the geometric pressure inside the pipe through which the liquid flows, which is determined by the following equation, Pa;

$$P_k = \rho g H \quad (13)$$

where ρ – liquid density, kg/m³; g – free fall acceleration, m/sec²; H – fluid level height, m;

P_{sh} – is the lost pressure at the outflow of the liquid from the hole, which is determined by the Darcy-Weisbach equation, Pa;

$$P_{sh} = \xi_{sh} \frac{v_s^2 \cdot \rho_s}{2} \quad (14)$$

where v_s – the rate at which fluid flows out of the hole, m/sec; ξ_{sh} – is the coefficient of resistance at which the liquid flows out of the nozzle hole, which is the thickness of the nozzle hole δ and diameter of hole d_{sh} .

Applying Bernoulli's law to equation (12), we assume that the pressure in the pipe is equal to P_k and the pressure in the nozzle hole is equal to P_{sh} . Then equation (12) can be written in the following form, Pa;

$$\rho_s g H = \xi_{sh} \frac{v_s^2 \cdot \rho_s}{2} \quad (15)$$

From the resulting equation (15) we determine the velocity of the liquid, m/s;

$$v_s = \sqrt{\frac{2gH}{\xi_{sh}}} \quad (16)$$

From equation (16) we are able to determine the velocity of the liquid in the device. The fluid flow rate through the nozzle hole in the device is determined by the following equation, m³/h;

$$Q_s = 3600\pi R^2 \sqrt{\frac{2gH}{\xi_{sh}}} \quad (17)$$

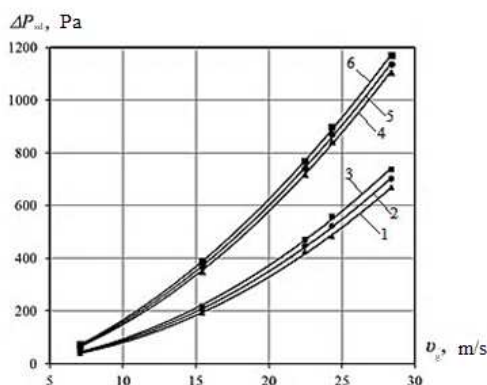
The results of experiments

The values of the variable factors for determining the hydraulic resistance of the device are fluid flow $Q_s=0,07\div 0,253$; $Q_s=0,071\div 0,295$; $Q_s=0,072\div 0,327$ m³/h, diameter of connecting pipe $d_{sh}=2; 2,5$ and 3 mm, gas velocity from $v_g=7,07$ m/s to 28,37 m/s intermediate step 4 m/s, the slope of the working body of the contact element, which gives a flexible motion to the gas flow $\alpha=30^\circ; 45^\circ$ and 60° [10,11]. Quartz sand and dolomite dust were used in the experiments. Laboratory analyzes were performed to determine the dispersed composition of the dust [12]. According to him, quartz sand is for a mixture of dust and gas $\rho_{ar}=1,89$ kg/m³ and compounds of dolomite dust and gas equals $\rho_{ar}=2,13$ kg/m³. 1m³ he amount of dust in the air according to STATE STANDARD-22551-77 for quartz dust 345,4 mg/m³, and according to State standard-23672-79 for dolomite dust 360,3 mg/m³ [13,14,15]. In the device, the local resistance coefficient at the distance from the inlet pipe of the dusty gas to the device and the contact element forming the coil is assumed to be 0,7 [7]. The resistance coefficient in the contact element was determined experimentally for different

values of the variable factors. According to that, the angle of inclination of the surface through which the gas flow passes $\sin\beta=60^\circ$ the coefficient of resistance of the contact element when $\zeta=1,1$ and correction coefficient $\Delta k=0,91$; the angle of inclination of the surface through which the gas flow passes $\sin\beta=45^\circ$ the coefficient of resistance of the contact element when $\zeta=1,3$ and correlation coefficient $\Delta k=0,81$ and the angle of inclination of the surface through which the gas flows $\sin\beta=30^\circ$ the coefficient of resistance of the contact element when $\zeta=1,5$ and correlation coefficient $\Delta k=0,68$ were determined.

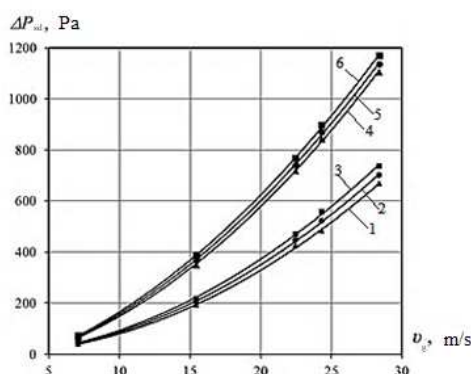
In this case $\sin\beta=60^\circ$, the total resistance coefficient of the device is the angle of inclination of the surface through which the gas flow passes equals 1,8; $\sin\beta=45^\circ$ equals 2 and $\sin\beta=30^\circ$ equals 2,2 were experimentally determined.

Experiments to determine the hydraulic resistance of the device were carried out in two stages. In the first stage, the effect of a mixture of quartz sand dust and air on the hydraulic resistance of the device was studied. The results of the experiments are shown in Figures 3, 4 and 5.



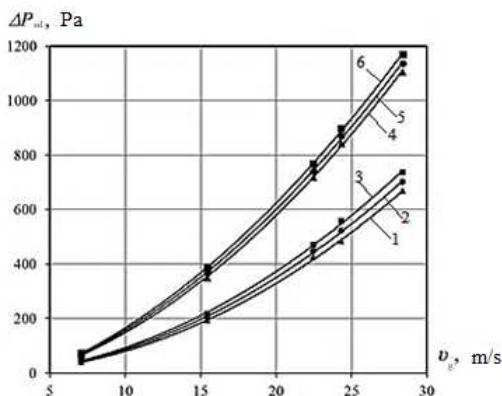
the reference angle of the contact element that moves the gas flow $\alpha=60^\circ$ and $\rho_g=1,89 \text{ kg/m}^3$ – const

Figure 3.



the reference angle of the contact element that moves the gas flow $\alpha=45^\circ$ and $\rho_g=1,89 \text{ kg/m}^3$ – const

Figure 4.



the reference angle of the contact element that moves the gas flow $\alpha=30^\circ$ and $\rho_g=1,89 \text{ kg/m}^3$ – const

Figure 5.

In 1 – $d_{sh}=2 \text{ mm}$ $Q_s=0,07 \text{ m}^3/\text{h}$; in 2 – $d_{sh}=2,5 \text{ mm}$ $Q_s=0,071 \text{ m}^3/\text{h}$; in 3 – $d_{sh}=3 \text{ mm}$ $Q_s=0,072 \text{ m}^3/\text{h}$; in 4 – $d_{sh}=2 \text{ mm}$ $Q_s=0,253 \text{ m}^3/\text{h}$; in 5 – $d_{sh}=2,5 \text{ mm}$ $Q_s=0,295 \text{ m}^3/\text{h}$; in 6 – $d_{sh}=3 \text{ mm}$ $Q_s=0,327 \text{ m}^3/\text{h}$;
Figure 3; 4 and 5. Dependence of hydraulic resistance the fluid-supplied device ΔP_{sd} on the gas velocity v_g

Figures 3 – 5 show the effect of a mixture of gas and quartz sand dust on the hydraulic resistance. The data show that the gas velocity by $v_g=7,07 \div 28,37 \text{ m/sec}$ intermediate step 4 m/sec and the slope of the working body of the contact element, which provides a reciprocating motion to the gas flow $\alpha=30^\circ$; For 45° and 60° of the hydraulic resistance is the lowest and high load, minimum values of fluid consumption $d_{sh}=2 \text{ mm}$, $Q_s=0,07 \text{ m}^3/\text{h}$ – const for $P_{sd}=668 \text{ Pa}$ increased to 910 Pa. Intermediate step is $\alpha=30^\circ$ and 45° in the working surface equals to $\Delta P_{sd}=106 \text{ Pa}$, in $\alpha=45^\circ$ and 60° equals $\Delta P_{sd}=136 \text{ Pa}$. For $d_{sh}=2,5 \text{ mm}$, $Q_s=0,071 \text{ m}^3/\text{h}$ – const hdyrolic resistance was increased from $\Delta P_{sd}=702 \text{ Pa}$ to 970 Pa. Inermediate step is $\alpha=30^\circ$ and $\alpha=45^\circ$ among working surfaces $\Delta P_{sd}=127 \text{ Pa}$, $\alpha=45^\circ$ and $\alpha=60^\circ$ equals to $\Delta P_{sd}=141 \text{ Pa}$. For $d_{sh}=3 \text{ mm}$, $Q_s=0,072 \text{ m}^3/\text{h}$ – const hdyrolic resistance has been observed increase form $\Delta P_{sd}=737 \text{ Pa}$ to 1036 Pa. Intermediate steps are $\alpha=30^\circ$ and $\alpha=45^\circ$ among working surfaces hdyrolic resistance is $\Delta P_{sd}=153 \text{ Pa}$, in $\alpha=45^\circ$ and $\alpha=60^\circ$ hdyrolic resistance is $\Delta P_{sd}=146 \text{ Pa}$.

High load of hydraulic resistance was observed from $\Delta P_{sd}=1106$ Pa to 1425 Pa for maximum values of fluid flow $d_{sh}=2$ mm, $Q_s=0,253$ m³/h – const. The intermediate step was $\Delta P_{sd}=153$ Pa between the values of $\alpha=30^\circ$ and $\alpha=45^\circ$ working surface, while $\Delta P_{sd}=166$ Pa between the values of $\alpha=45^\circ$ and $\alpha=60^\circ$. $d_{sh}=2,5$ mm, $Q_s=0,295$ m³/h – const for $\Delta P_{sd}=1136$ Pa to 1502 Pa.

The intermediate step was $\Delta P_{sd}=197$ Pa between the values of $\alpha=30^\circ$ and $\alpha=45^\circ$ working surface, while the values between $\alpha=45^\circ$ and $\alpha=60^\circ$ were $\Delta P_{sd}=169$ Pa, and $d_{sh}=3$ mm, $Q_s=0,327$ m³/h. An increase in $\Delta P_{sd}=1170$ Pa to 1574 Pa was observed for – const. The intermediate step was $\Delta P_{sd}=220$ Pa between the values of $\alpha=30^\circ$ and $\alpha=45^\circ$ working surface, while $\Delta P_{sd}=184$ Pa between the values of $\alpha=45^\circ$ and $\alpha=60^\circ$.

The intermediate step was $\Delta P_{sd}=197$ Pa between the values of 30° and $\alpha=45^\circ$ working surface, while the values between $\alpha=45^\circ$ and 60° were $\Delta P_{sd}=169$ Pa, and $d_{sh}=3$ mm, $Q_s=0,327$ m³/h an increase in $\Delta P_{sd}=1170$ Pa to 1574 Pa was observed for – const. The intermediate step was $\Delta P_{sd}=220$ Pa between the values of $\alpha=30^\circ$ and $\alpha=45^\circ$ working surface, while $\Delta P_{sd}=184$ Pa between the values of $\alpha=45^\circ$ and $\alpha=60^\circ$.

The following empirical formulas were obtained using the least squares method for the graphical dependencies shown in Figures 3; 4 and 5 [13,15].

The results in angle of $\alpha = 60^\circ$ – const

$$y = 0,8468x^2 - 0,4903x + 0,436R^2 = 0,9996 \quad (18)$$

$$y = 0,8691x^2 + 0,302x - 3,0465R^2 = 0,9998(19)$$

$$y = 0,8859x^2 + 1,3697x - 9,0306R^2 = 0,9993(20)$$

$$y = 1,1181x^2 + 9,4488x - 57,21R^2 = 0,9998(21)$$

$$y = 1,0916x^2 + 11,641x - 68,262R^2 = 0,9998(22)$$

$$y = 1,0756x^2 + 13,601x - 77,946R^2 = 0,9998(23)$$

The results in angle of $\alpha = 45^\circ$ – const

$$y = 0,9056x^2 + 3,9202x - 25,503R^2 = 0,9983(24)$$

$$y = 0,9235x^2 + 4,802x - 28,392R^2 = 0,9992(25)$$

$$y = 0,9302x^2 + 6,0296x - 33,118R^2 = 0,9997(26)$$

$$y = 1,2453x^2 + 12,519x - 77,957R^2 = 0,9997(27)$$

$$y = 1,2643x^2 + 13,017x - 74,367R^2 = 0,9997(28)$$

$$y = 1,2542x^2 + 15,044x - 78,952R^2 = 0,9999(29)$$

The results in angle of $\alpha = 30^\circ$ – const

$$y = 1,0743x^2 + 2,9391x - 22,428R^2 = 0,9972(30)$$

$$y = 0,9876x^2 + 8,4388x - 49,312R^2 = 0,9975(31)$$

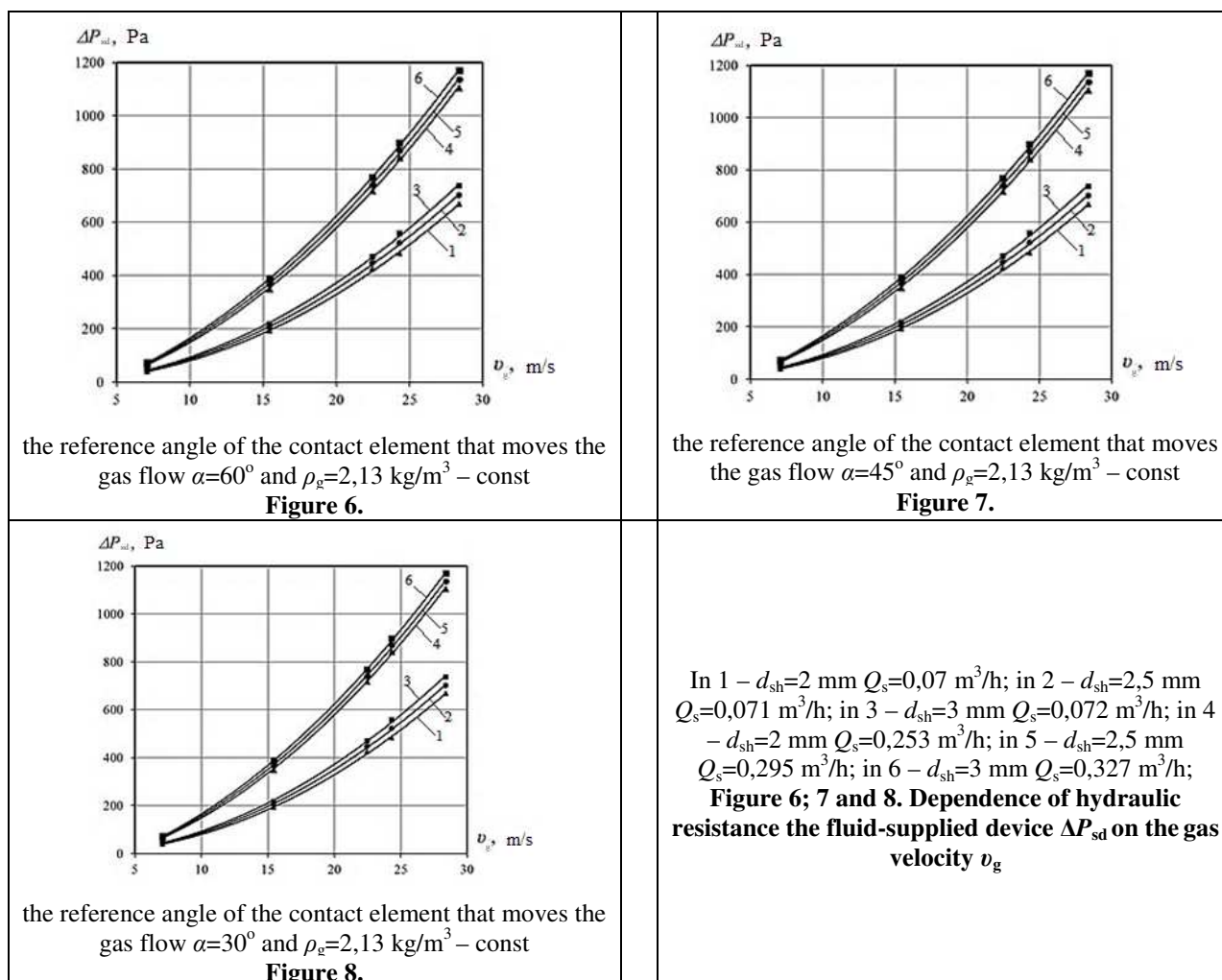
$$y = 0,9808x^2 + 10,967x - 55,717R^2 = 0,9986(32)$$

$$y = 1,197x^2 + 21,567x - 129,93R^2 = 0,9981(33)$$

$$y = 1,1793x^2 + 24,901x - 141,53R^2 = 0,9994(34)$$

$$y = 1,1289x^2 + 28,985x - 152,25R^2 = 0,9998(35)$$

In the second stage, the effect of a mixture of dolomite dust and air on the hydraulic resistance of the device was studied. The results of the experiments are shown in Figures 6; 7 and 8.



Figures 6 - 8 show the effect of a mixture of gas and dolomite dust on the hydraulic resistance. The data show that the gas velocity $v_g=7,07\div 28,37 \text{ m/s}$ with an intermediate step of 4 m/s and the minimum and maximum load of hydraulic resistance for the working body slope $\alpha=30^\circ$; 45° and 60° of the contact element moving in the gas flow, the minimum values of fluid consumption $d_{sh}=2 \text{ mm}$, $Q_s=0,07 \text{ m}^3/\text{h}$ – const for $\Delta P_c=749 \text{ Pa}$ increased to 1036 Pa.

The intermediate step was $\Delta P_{sd}=134 \text{ Pa}$ between the values of $\alpha=30^\circ$ and 45° working surface, while $\Delta P_{sd}=153 \text{ Pa}$ between the values of $\alpha=45^\circ$ and $\alpha=60^\circ$ $d_{sh}=2,5 \text{ mm}$, $Q_s=0,071 \text{ m}^3/\text{h}$ – const for $\Delta P_{sd}=787 \text{ Pa}$ to 1088 Pa. The intermediate step was $\Delta P_{sd}=142 \text{ Pa}$ between the values of the working surface $\alpha=30^\circ$ and $\alpha=45^\circ$, while the values between $\alpha=45^\circ$ and $\alpha=60^\circ$ were $\Delta P_{sd}=159 \text{ Pa}$ and $d_{sh}=3 \text{ mm}$, $Q_s=0,072 \text{ m}^3/\text{h}$ An increase in $\Delta P_{sd}=826 \text{ Pa}$ to 1140 Pa was observed for – const. The intermediate step was $\Delta P_{sd}=149 \text{ Pa}$ between the values of $\alpha=30^\circ$ and $\alpha=45^\circ$ of the working surface, while $\Delta P_{sd}=165 \text{ Pa}$ between the values of $\alpha=45^\circ$ and $\alpha=60^\circ$.

High load of hydraulic resistance, increase in $\Delta P_{sd}=1240 \text{ Pa}$ to 1615 Pa for maximum values of fluid flow $d_{sh}=2 \text{ mm}$, $Q_s=0,253 \text{ m}^3/\text{h}$ – const were observed. The intermediate step was $\Delta P_{sd}=188 \text{ Pa}$ between the values of $\alpha=30^\circ$ and $\alpha=45^\circ$ working surface, while $\Delta P_{sd}=187 \text{ Pa}$ between the values of $\alpha=45^\circ$ and $\alpha=60^\circ$. $d_{sh}=2,5 \text{ mm}$, $Q_s=0,295 \text{ m}^3/\text{h}$ – const for $\Delta P_{sd}=1275 \text{ Pa}$ to 1656 Pa. The intermediate step was $\Delta P_{sd}=192 \text{ Pa}$ between the values of $\alpha=30^\circ$ and $\alpha=45^\circ$ working surface, while $\Delta P_{sd}=189 \text{ Pa}$ between $\alpha=45^\circ$ and $\alpha=60^\circ$, and $d_{sh}=3 \text{ mm}$, $Q_s=0,327 \text{ m}^3/\text{h}$ An increase in $\Delta P_{sd}=1312 \text{ Pa}$ to 1697 Pa was observed for – const. The intermediate step was $\Delta P_{sd}=195 \text{ Pa}$ between the values of $\alpha=30^\circ$ and $\alpha=45^\circ$ working surfaces, while $\Delta P_{sd}=190 \text{ Pa}$ between the values of $\alpha=45^\circ$ and $\alpha=60^\circ$.

The following empirical formulas were obtained using the least squares method for the graphical dependencies shown in Figures 6; 7 and 8 [13].

The results in angle of $\alpha = 60^\circ$ – const

$$y = 0,9531x^2 - 0,6803x + 1,3647R^2 = 0,9996(36)$$

$$y = 0,9705x^2 + 0,4993x - 4,6903R^2 = 0,9998(37)$$

$$y = 0,9993x^2 + 1,3433x - 8,7918R^2 = 0,9993(38)$$

$$y = 1,2494x^2 + 10,749x - 65,144R^2 = 0,9998(39)$$

$$y = 1,2274x^2 + 12,964x - 75,565R^2 = 0,9998(40)$$

$$y = 1,2124x^2 + 15,056x - 86,085R^2 = 0,9999(41)$$

The results in angle of $\alpha = 45^\circ$ – const

$$y = 1,0216x^2 + 4,183x - 26,853R^2 = 0,9983(42)$$

$$y = 1,0316x^2 + 5,5053x - 32,278R^2 = 0,9992(43)$$

$$y = 1,0452x^2 + 6,7077x - 36,746R^2 = 0,9997(44)$$

$$y = 1,4028x^2 + 13,785x - 85,066R^2 = 0,9997(45)$$

$$y = 1,4193x^2 + 14,545x - 83,152R^2 = 0,9997(46)$$

$$y = 1,437x^2 + 15,34x - 82,431R^2 = 0,9998(47)$$

The results in angle of $\alpha = 30^\circ$ – const

$$y = 1,1097x^2 + 8,0011x - 59,241R^2 = 0,9944(48)$$

$$y = 1,0071x^2 + 13,288x - 80,005R^2 = 0,9968(49)$$

$$y = 0,8751x^2 + 19,624x - 106,76R^2 = 0,9984(50)$$

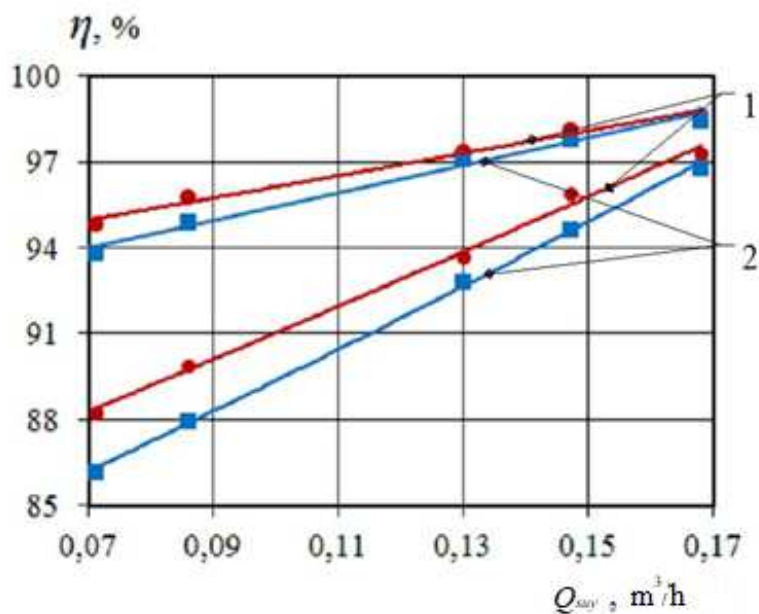
$$y = 1,4413x^2 + 21,287x - 129,08R^2 = 0,9985(51)$$

$$y = 1,4405x^2 + 22,764x - 131,21R^2 = 0,9987(52)$$

$$y = 1,4116x^2 + 25,327x - 138,01R^2 = 0,9987(53)$$

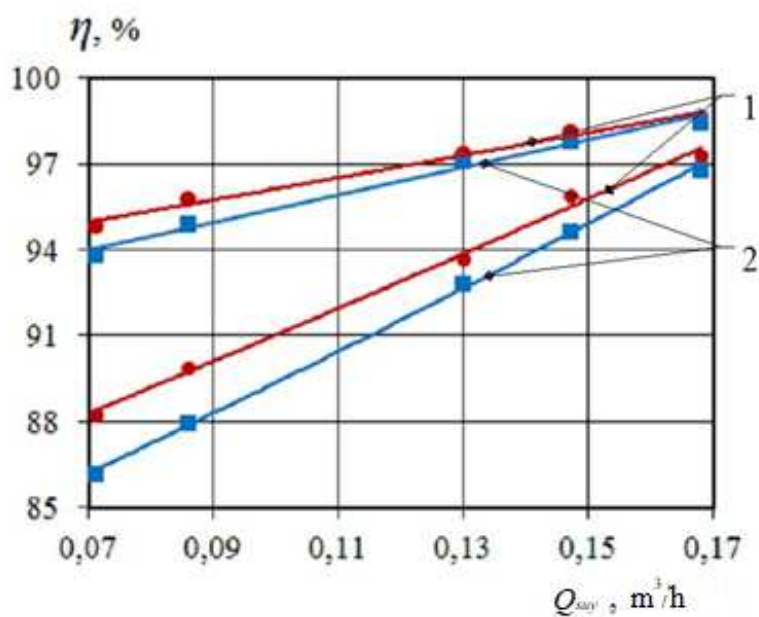
The results of experiments on the determination of hydraulic resistance and the research work of K.T.Semrau [18] were used to study the cleaning efficiency of the device. It is known from the research work of K.T.Semrau that the cleaning efficiency depends on the hydraulic resistance of the device. In this case, the total energy consumption should be spent on the purification of dusty gases using liquids [16,17]. Based on the above, the effect of hardware hydraulic resistance on cleaning efficiency was investigated.

In the experiments, the following limits of the variables, the diameter of the fluid nozzle $d_{sh}=2; 2,5$ and 3 mm, the fluid consumption $Q_s=0,070\div 0,295$ m³/h increased the interval to $0,060$ m³/h, the contact element blades mounted on the working pipe slope angle $\alpha=30^\circ$; The number of blades mounted on the contact element 45° and 60° was increased to [15], the gas velocity $v_g=5\div 25$ m/s, the intermediate step was increased to 5 m/s. Gas density $\rho_g=1,89$ kg/m³ for a mixture of air and quartz sand powder, $\rho_g=2,13$ kg/m³ for a mixture of air and dolomite dust, 4 mg/m³ and dolomite powder was determined at the request of PDK and $360,3$ mg/m³ in accordance with GOST-23672-79). The temperature for the water and gas system was set at 20 °S ± 2 , taking into account the influence of the external environment during the experiments. Based on the results of the experiments, comparison graphs were constructed on the effect of hydraulic resistance on the cleaning efficiency. (Figures 9-11). Given the multivariate nature of the experiments, the graphs were constructed for different values of fluid consumption and for low and high gas velocity loads.



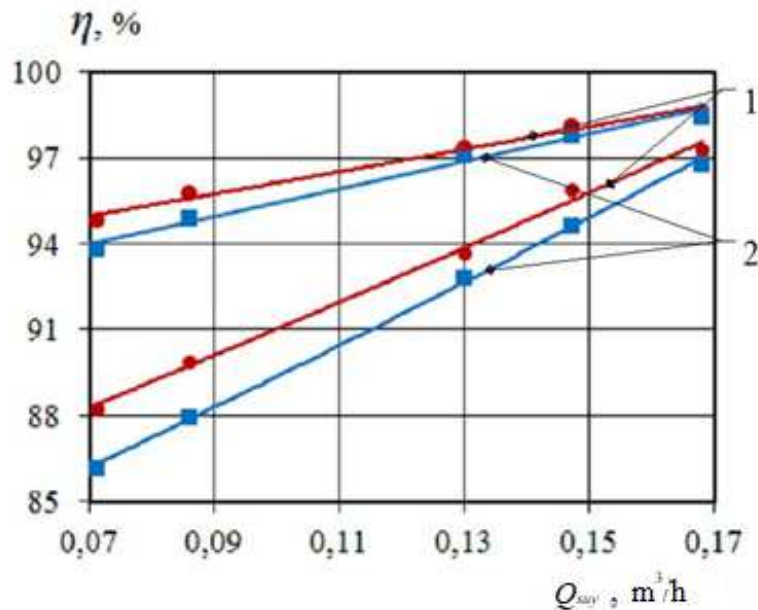
1 – quartz sand powder; 2 – dolomite dust

Figure 9. The dependence of the cleaning efficiency η on the liquid consumption Q_s , $\alpha=60^\circ$ – const.



1 – quartz sand powder; 2 – dolomite dust

Figure 10. The dependence of the cleaning efficiency η on the liquid consumption Q_s , $\alpha=45^\circ$ – const.



1 – quartz sand powder; 2 – dolomite dust

Figure 11. The dependence of the cleaning efficiency η on the liquid consumption Q_s $\alpha=30^\circ$ – const.

From the data given in Figures 9-11 it can be seen that the angle of inclination of the contact element blades mounted on the working pipe is $\alpha=60^\circ$, liquid consumption $Q_s=0,070\div 0,295$ m³/h for the lower limit of gas velocity. dolomite dust removal efficiency was 86,17÷96,81 %, quartz sand dust removal efficiency for the upper gas velocity limit was 94,81÷98,62 % and dolomite dust removal efficiency was 93,81÷98,43 %.

Slope angle of contact element blades $\alpha=45^\circ$, liquid consumption $Q_s=0,070\div 0,295$ m³/h for the lower limit of gas velocity, quartz sand dust cleaning efficiency 90,28÷97,65 % and dolomite dust cleaning efficiency 88,13÷97,21 %, the efficiency of quartz sand dust removal for the upper limit of gas velocity was 95,6÷98,99 % and the efficiency of dolomite dust removal was 94,99÷98,76 %.

Slope angle of contact element blades $\alpha=30^\circ$, liquid consumption $Q_s=0,070 \div 0,295$ m³/h for the lower limit of gas velocity quartz sand dust cleaning efficiency 92,65÷98,9 % and dolomite dust cleaning efficiency 91,4÷98,21 %, the efficiency of quartz sand dust removal for the upper limit of gas velocity was 96,7÷99,9 % and the efficiency of dolomite dust removal was 96,13÷99,8 %.

The following empirical formulas were obtained using the least squares method for the graphical dependencies shown in Figures 9-11 [19]:

When the angle of inclination of the contact element blades mounted on the working pipe is $\alpha=60^\circ$,

$$1) y = 79,208e^{1,205x} R^2 = 0,9991(54)$$

$$2) y = 82,201e^{1,0186x} R^2 = 0,9951(55)$$

$$3) y = 90,766e^{0,4993x} R^2 = 0,9857(56)$$

$$4) y = 92,315e^{0,4036x} R^2 = 0,9888(57)$$

When the angle of inclination of the contact element blades mounted on the working pipe $\alpha=45^\circ$;

$$1) y = 81,695e^{1,0239x} R^2 = 0,9964(58)$$

$$2) y = 85,682e^{0,7797x} R^2 = 0,9936(59)$$

$$3) y = 92,114e^{0,423x} R^2 = 0,993(60)$$

$$4) y = 92,915e^{0,3927x} R^2 = 0,9794(61)$$

When the angle of inclination of the contact element blades mounted on the working pipe $\alpha=30^\circ$;

$$1) y = 86,537e^{0,7716x} R^2 = 0,9877(62)$$

$$2) y = 88,182e^{0,6772x} R^2 = 0,9923(63)$$

$$3) y = 94,141e^{0,3535x} R^2 = 0,9915(64)$$

$$4) y = 94,585e^{0,3337x} R^2 = 0,9899(65)$$

Conclusion

From the experiments conducted to determine the hydraulic resistance and study its effect on the cleaning efficiency, it can be concluded that the increase in the reference angle of the contact element moving in the gas flow in the device provided thickening of the liquid film layer. But it led to a decrease in the working surface. Conversely, a decrease in the reference angle resulted in a thinning of the liquid film layer and an increase in the working surface. This in turn led to an increase in hydraulic resistance. In addition, changes in the velocity and density of the gas supplied to the device also have a significant effect on the hydraulic resistance. As a result of the increase in hydraulic resistance, the cleaning efficiency has improved, but the energy consumption used to clean the dusty gas has increased. Therefore, it is important to achieve maximum cleaning efficiency at minimum values of hydraulic resistance [20,21]. As can be seen from the graphs, the cleaning efficiency of quartz sand dust is higher than that of dolomite dust, which can be explained by the differences in the average median sizes of the dust samples. When designing the industrial variant of the device, it is recommended to take into account the average median size of the dust emitted from industrial plants.

References:

1. Валдберг А.Ю., Николайкина Н.Е. Процесс и аппараты защиты окружающей среды. – Москва: Дрофа, 2008. – 239 с.
2. Алиев Г.М. Устройство и обслуживание газоочистных и пыле-улавливающих установок. – Москва: Металлургия, 1988. – 367 с.
3. Сугак Е.В., Войнов Н.А., Николаев Н.А. Очистка газовых выбросов в аппараты с интенсивными гидродинамическими режимами. – Кемерово: Школа, 1999. – 224 с.
4. Усманова Р.Р. Повышение эффективности газоочистки в инерционных аппаратах с активной гидродинамикой. Дисс... док. техн. наук. – Уфа, 2017, – 171-180 с.
5. Нечаева Е.С. Исследование основных характеристик роторного распылительного пылеуловителя. Дисс ... канд. техн. наук. – Кемерово, 2014, – 149 с.
6. Эргашев Н.А., Алиматов Б.А., Каримов И.Т. Контакт элементи буралган йўлдош қуюнли режимда ишловчи ҳўл усулда чанг тозаловчи аппарат // Фарғона политехника институтининг илмий-техник журнали. – Фарғона, 2019. – №2. – Б. 147-152.
7. Латипов К.Ш. Гидравлика, гидромашиналар ва гидроюритмалар. – Тошкент: Ўқитувчи, 1992. – 405 б.
8. Салимов З. Кимёвий технологиянинг асосий жараёнлари ва қурилмалари. Том-1. – Тошкент: Ўзбекистон, 1994. – 366 б.
9. Эргашев Н.А. Исследование гидравлического сопротивления пылеулавливающего устройства мокрым способом // Universum. – Москва, 2019. – № 12 (69). – С. 59-62.
10. Эргашев Н.А., Алиматов Б.А., Хошимов Ж.Н. Ҳўл усулда чанг ва газларни тозаловчи аппаратга берилётган суюқлик сарфини тажрибавий аниқлаш // “Кимё, қурилиш материаллари саноати ҳамда турдош ишлаб чиқариш соҳаларига инновацион техника ва технологияларни жорий этишнинг долзарб муаммолари” мавзусида I-Халқаро илмий-амалий анжумани 2019. – Б. 351-352.
11. Эргашев Н.А., Маткаримов Ш.А., Зияев А.Т., Тожибоев Б.Т., Қўчқоров Б.У. Опытное определение расхода газа, подаваемое на пылеочищающую установку с контактным элементом, работающим в режиме спутникового вихря // Universum. – Москва, 2019. – № 12 (69). – С. 54-58.
12. Эргашев Н.А., Алиматов Б.А., Ахунбаев А.А. Намуна учун танланган чангларнинг дисперс таркибини тажрибавий аниқлаш // Global science and innovations 2019: Central Asia материалы V-Международной научно-практической конференции. – Астана, 2019. – С. 276-279.
13. ГОСТ 23672-79 Доломит для стекольной промышленности. Технические условия. – Москва: Стандартиформ, 1979. – 14 с.
14. Кобзарь А.И. Прикладная математическая статистика. Для инженеров и научных работников.–Москва: Физматлит, 2006.– 816 с.

15. Ergashev N.A., Isomidinov A.S., Alimatov B.A. Determination hydraulic resistance of device that has the vortex flow creating contact element // Austrian journal of technical and natural sciences. – Vienna. 2020. – № 3-4. – P.15-22.
16. Эргашев Н.А. Научно-технические основы использования в промышленности аппарата для мокрого пылеулавливания и газоочистки. Дисс. ...PhD. – Ташкент, 2021. –116 с.
17. Эргашев Н.А., Алиматов Б.А., Қўчқоров Б. Контакт элементи буралган йўлдош қуюнли режимда ишловчи ҳўл усулда чанг тозаловчи қурилмага берилаетган газ сарфини тажрибавий аниқлаш // Машинасозлик ишлаб чиқариш ва таълим муаммолари ва инновацион ечимлар: Республика илмий-техник анжумани–Фарғона, 2019. – Б. 315-318.
18. B.O. Andersen, N.F.Nielsen, J.H. Walthe. Numerical and experimental study of pulse-jet cleaning in fabric filters // Powder Technology. – Netherlands, 2016. – 291, – pp. 284-298.
19. Эргашев Н.А., Алиматов Б.А. Контакт элементи буралган йўлдош - қуюнли режимда ишловчи ҳўл усулда чанг тозаловчи қурилмада гидравлик қаршиликларни тажрибавий аниқлаш // Фарғона политехника институтининг илмий-техник журнали. – Фарғона, 2020. – №2. – Б. 182-184.
20. Касаткин А.Г., Основные процессы и аппараты химической технологии. – Москва: Химической литературы Часть – 1, 1948. – 948 с.
21. Исомидинов А.С. Разработка эффективных методов и устройств очистки пылевых газов химической промышленности: Дисс. ... PhD. – Ташкент, 2020. – 118 с.
22. Халилов Ш. З., Гаппаров К. Г., Махмудов И. Р. Влияние травмирования и способов обмолота семян пшеницы на их биологические и урожайные свойства //Журнал Технических исследований. – 2020. – Т. 3. – №. 1.
23. Namzaev, K Gapparov, E Umarov, Z Abdullaev Building and architecture//Universum: Технические науки. - 2021.-Т -3 (84).